Modeling of the Electric Field-Induced Birefringence of Vesicles

Viktor Peikov and Zoltan A. Schelly*

Center for Colloidal and Interfacial Dynamics, Department of Chemistry and Biochemistry, University of Texas at Arlington, Arlington, Texas 76019-0065

Received: October 2, 2003; In Final Form: March 17, 2004

Electric birefringence of unilamellar lipid vesicles, elongated in the direction of the applied field **E**, is modeled for a low degree of deformation to a prolate ellipsoid of the original spherical shells. The existing theory for water-in-oil microemulsion is adapted, and the intrinsic birefringence of the lipid membrane and the form birefringence of the aqueous inner compartment of the vesicle are taken into account. Deformation under both constant surface area and constant volume conditions are considered, but thinning of the bilayer at the polar caps and rotational/orientational effects are neglected. For illustration of the utility of the theoretical results, the extent of elongation of large unilamellar vesicles (LUV), prepared from the zwitterionic DOPC (dioleoylphosphatidylcholine), is calculated based on available experimentally measured induced birefringence data. With the use of reasonable values for the refractive indexes of the membrane, the axial ratio P of the deformed vesicle is found to be in the range of 1.02−1.07. The equations derived are also suitable for calculation of the bending elasticity modulus κ of the bilayer from *experimentally* determined values of the Kerr constant K, provided the electrical and optical properties of the vesicle membrane are known.

Introduction

Electrooptic methods (birefringence, dichroism, and turbidity induced by an external electric field) have often been used as effective tools for studying structural properties, dynamic behavior, stability, and phase transitions in organized assemblies such as microemulsions, liquid crystals, and synthetic unilamellar bilayer vesicles.[1−16] Despite the abundance of experimental studies, the theory of electrooptic effects of vesicles has not been sufficiently advanced. In the absence of an external force field, vesicles and microdroplets undergo continuous thermal shape fluctuations[17] but their time average shape is usually spherical. It is generally accepted that the electrooptic effects observed on originally spherical vesicles are mainly due to the field-induced polarization and deformation of the bilayer shell to a prolate ellipsoid of revolution with its major axis parallel to the applied field **E**. Electrostrictive thinning of the membrane at the polar caps[1] and the rotational alignment of induced[4] and instantaneous[14] dipoles may also contribute to the effects. The theory of deformation of spherical vesicles with isotropic nonconducting or conducting membrane at low-intensity ac and dc electric fields was developed by Helfrich and co-workers,[18−20] and was later extended to high field strengths by Hyuga et al. by the use of perturbation theory.[21−23]

Anisometric particles are expected to exhibit electric birefringence ("form birefringence") if their refractive index differs from that of the medium.[24] Thus, the total birefringence of the system will be a sum of the form birefringence and any intrinsic birefringence arising from the intrinsic optical anisotropy of the particles. The theory of electric birefringence of deformable particles at low electric fields (Kerr region) was developed by Borkovec and Eicke.[5] They calculated the polarizability and the birefringence of water-in-oil microemulsion droplets in the ellipsoidal shape fluctuation approximation and obtained the surfactant monolayer's bending rigidity κ from electric birefringence experimental data.[6] Van der Linden et al.[25] extended the theoretical treatment by taking into account the birefringence of the surfactant monolayer at the water/oil interface, based on Helfrich's approach to describing the magnetic birefringence of vesicles.[26]

In the present paper, van der Linden et al.'s theoretical treatment of microemulsions is modified and extended to accommodate the case of vesicles. In the equations derived here, both the intrinsic birefringence of the lipid membrane and the form birefringence of the inner aqueous compartment of the vesicle are taken into account. Experimental electric birefringence data obtained previously[14,16] are used to calculate the extent of elongation of large unilamellar bilayer vesicles (LUV) prepared from the zwitterionic phospholipid dioleoylphosphatidylcholine (DOPC; 1,2-dioleoyl-*sn*-glycero-3-phosphocholine).

Theory

Electric birefringence of a completely oriented disperse system, that is, the saturation birefringence Δn_s, arises from the difference in optical polarizabilities of the dispersed phase parallel ($\alpha^\circ_{||}$) and perpendicular ($\alpha^\circ_{\perp}$) to the applied electric field **E**:[27]

$$\Delta n_s \equiv n_{||} - n_{\perp} = N(\alpha^\circ_{||} - \alpha^\circ_{\perp})/2n \qquad (1)$$

where N is the number concentration of dispersed particles and n is the refractive index of the isotropic (unoriented) system.

To calculate the electric birefringence of vesicles the following one-shell model is used (Figure 1). (A similar one-shell model, but with radially oriented optically anisotropic elements, was also used for modeling the Mie scattering of vesicles.[28]) We assume the vesicles to have spherical initial shape with inner radius R_0 and a homogeneous bilayer of thickness D, $D \ll R_0$. The applied homogeneous electric field **E** is assumed to cause only a slight deformation of the vesicle to a prolate ellipsoid with its major axis parallel to the field. Possible thinning of the

* Corresponding author. E-mail: schelly@uta.edu.

10.1021/jp0369488 CCC: $27.50 © 2004 American Chemical Society
Published on Web 06/09/2004

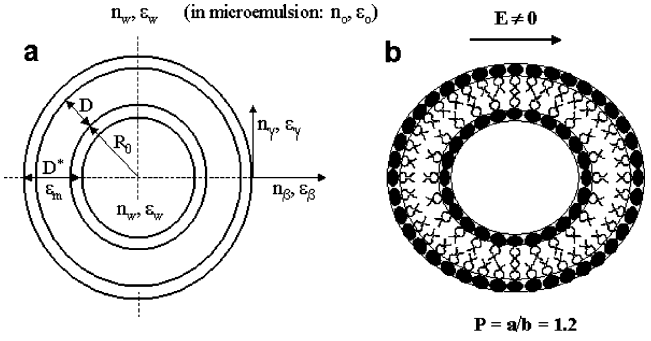

Figure 1. Schematic model of a lipid vesicle: (a) no field applied, $E = 0$; (b) electric field of strength E is applied. See the text for explanation of the symbols.

lipid bilayer and rotational/orientational effects are neglected. With analogous assumptions, the electric polarizability of a water-in-oil microemulsion droplet is given by[25]

$$\alpha_i = V(\epsilon_w - \epsilon_o)\left[\frac{\epsilon_o}{\epsilon_o + L_i(\epsilon_w - \epsilon_o)}\right] + O\left[\frac{\epsilon_o}{\epsilon_o + L_i(\epsilon_w - \epsilon_o)}\right]^2 [\epsilon_w{}^2\beta\overline{\vec{n}\,\vec{n}}^s + \gamma\overline{(1 - \vec{n}\,\vec{n})}^s] \quad (2)$$

where $i = \parallel$ or $\perp$ denotes direction with respect to the applied electric field **E**, $V = 4ab^2/3$ is the volume, and $O = 2\pi[b^2 + (ab/e)\arcsin e]$ is the surface area of the aqueous pool of the ellipsoidally deformed droplet; ϵ_w and ϵ_o are dielectric constants of the droplet (water) and of the medium (oil), $\vec{n}$ is the normal to the surface, $\overline{.....}^s$ indicates an average over the surface, and a, b, and $e = (1 - (b/a)^2)^{1/2}$ are the major semiaxis, minor semiaxis, and eccentricity of the droplet, respectively. The depolarization factors L_i for prolate ellipsoid in eq 2 are given as[29]

$$L_\parallel = 1 - 2L_\perp = (1 - e^{-2})\left[1 - \frac{1}{2e}\ln\left(\frac{1+e}{1-e}\right)\right]$$

In eq 2, $\beta = D^*(\epsilon_o{}^{-1} - \epsilon_\beta{}^{-1})$ and $\gamma = D^*(\epsilon_\gamma - \epsilon_o)$ are the excess polarizabilities of the surfactant layer normal and tangential to the surface, respectively, expressed in terms of the normal (ϵ_β) and tangential (ϵ_γ) components of the dielectric constant and the thickness (D^*) of the membrane playing a role in the electric polarizability. Equation 2 can be adapted to describe the electric polarizabilities of vesicles by replacing ϵ_o by ϵ_w, since both the inner compartment and the external space are occupied by identical aqueous solutions (or by water in the case of nonionic or zwitterionic surfactants). The substitution ($\epsilon_o = \epsilon_w$) for vesicles yields

$$\alpha_i = O[\epsilon_w{}^2\beta\overline{\vec{n}\,\vec{n}}^s + \gamma\overline{(1 - \vec{n}\,\vec{n})}^s] \quad (3)$$

Deformation of an initially spherical object to a prolate ellipsoid is possible only if it is accompanied by a change of the volume or/and the surface area of the shell. Two different approximations have been used in the literature: deformation at constant volume[25] and deformation at constant surface area.[26] In the first case, the volume of the shell is assumed to remain constant throughout the deformation and the surface area is assumed to increase accordingly. This approximation is suitable for water-in-oil microemulsions[25] where free surfactant molecules from the nonpolar phase can enter and stabilize the increment of the water/oil interface. Such a possibility is moot for vesicles because of the virtual absence of free lipid molecules in the aqueous phase and the unstretchability of the membrane by moderate forces. Also, the membrane is permeable to water; hence, the volume of the enclosed fluid may adjust relatively freely. Thus, for vesicles, preference must be given to the constant surface area approximation. For small deformations, the volume or the surface area can be expanded in series of the eccentricity giving $V = 4\pi R_0{}^3/3$ and $O = 4\pi R_0{}^2[1 + (^2/_{45})e^4]$ in the case of constant volume,[25] or $V = (4\pi R_0{}^3/3)(1 - (^1/_{15})e^4)$ and $O = 4\pi R_0{}^2$ in the case of constant surface area.

Up to second order in the eccentricity, however, the two different approximations yield identical expressions for V or O, and consequently, the electric polarizabilities of microemulsion droplets are[25]

$$\alpha_\parallel = \frac{4\pi R_0{}^3}{3}(\epsilon_w - \epsilon_0)\left(\frac{3\epsilon_o}{\epsilon_w + 2\epsilon_o}\right)\left(1 + \frac{2}{5}e^2\left(\frac{\epsilon_w - \epsilon_o}{\epsilon_w + 2\epsilon_o}\right)\right) + \frac{4\pi R_0{}^2}{3}\left(\frac{3\epsilon_o}{\epsilon_w + 2\epsilon_o}\right)^2\left[\epsilon_w{}^2\beta\left(1 + \frac{4}{15}e^2\left(\frac{\epsilon_w - 7\epsilon_o}{\epsilon_w + 2\epsilon_o}\right)\right) + 2\gamma\left(1 + \frac{4}{15}e^2\left(\frac{4\epsilon_w - \epsilon_o}{\epsilon_w + 2\epsilon_o}\right)\right)\right] \quad (4)$$

$$\alpha_\perp = \frac{4\pi R_0{}^3}{3}(\epsilon_w - \epsilon_0)\left(\frac{3\epsilon_o}{\epsilon_w + 2\epsilon_o}\right)\left(1 - \frac{1}{5}e^2\left(\frac{\epsilon_w - \epsilon_o}{\epsilon_w + 2\epsilon_o}\right)\right) + \frac{4\pi R_0{}^2}{3}\left(\frac{3\epsilon_o}{\epsilon_w + 2\epsilon_o}\right)^2\left[\epsilon_w{}^2\beta\left(1 - \frac{2}{15}e^2\left(\frac{\epsilon_w - 7\epsilon_o}{\epsilon_w + 2\epsilon_o}\right)\right) + 2\gamma\left(1 - \frac{2}{15}e^2\left(\frac{4\epsilon_w - \epsilon_o}{\epsilon_w + 2\epsilon_o}\right)\right)\right] \quad (4')$$

In our case of vesicles ($\epsilon_o = \epsilon_w$), these result in

$$\alpha_\parallel = \frac{4\pi R_0{}^2}{3}\left[\epsilon_w{}^2\beta\left(1 - \frac{8}{15}e^2\right) + 2\gamma\left(1 + \frac{4}{15}e^2\right)\right] \quad (5)$$

$$\alpha_\perp = \frac{4\pi R_0{}^2}{3}\left[\epsilon_w{}^2\beta\left(1 + \frac{4}{15}e^2\right) + 2\gamma\left(1 - \frac{2}{15}e^2\right)\right] \quad (5')$$

These equations describe the optical polarizabilities ($\alpha^\circ_\parallel$ and $\alpha^\circ_\perp$) as well, since at optical frequencies $\epsilon_i = n_i{}^2$, where $i = w$, β, γ, o. With these, substitution of eqs 5 and 5′ into eq 1 yields the saturation birefringence for vesicles:

$$\Delta n_s = \frac{8N\pi R_0{}^2 D}{15 n_w}[(n_\gamma{}^2 - n_w{}^2) - n_w{}^4(n_w{}^{-2} - n_\beta{}^{-2})]e^2 \quad (6)$$

Here, D is used instead of D^* (see Figure 1) to take into account the relevance of the different thicknesses of the bilayer for the optical versus electrical polarizability. Also, in arriving at the last equation, n has been replaced with n_w (water) since the refractive index of dilute systems is approximately equal to that of the solvent.

Note that since rotational/orientational effects are neglected, the saturation birefringence Δn_s represents the steady-state birefringence measured in dilute solutions and will be referred to as such henceforth. Thus, from eq 6 we find the steady-state birefringence of vesicles to be linearly proportional to e^2 and to depend in a complex manner on the refractive indexes of the membrane and solvent.

The steady-state shape of the vesicle can be found by minimizing the total energy of deformation U of the lipid membrane.[26] Generally, U is a sum of the electrostatic energy U_E, curvature-elastic energy U_C, stretching energy U_S, and surface tension energy U_γ.[30] For microemulsions and lipid

bilayers U_S and U_γ can be neglected so that $U = U_E + U_C$. For small deformations, for example, up to the e^4 term, U_C has been calculated in the constant surface area approximation:[26]

$$U_C = 16\pi\mu kT\left[1 + \frac{2}{15}e^4 - R_0C_0\left(1 + \frac{1}{45}e^4\right) + \frac{1}{4}R_0^2C_0^2\right] \quad (7)$$

Here, C_0 is the spontaneous curvature of the bilayer, the dimensionless constant μ is linked to the elastic modulus of the membrane κ ($= 2\mu kT$),[26,31] and kT is the thermal energy. Assuming that both the polarization and deformation of the vesicles are in the field direction:

$$U_E = -\epsilon_0'\alpha_{||}E^2/2 \quad (8)$$

where ϵ_0' is the dielectric permeability of vacuum. By minimizing the total energy U as a function of the eccentricity e one can obtain an expression for the steady-state deformation of the vesicles at a constant electric field strength, both in the constant surface area and constant volume approximations:

$$e^2 = \frac{\epsilon_0'E^2R_0^2D^*}{\mu kT(12 - 2R_0C_0)}[(\epsilon_\gamma - \epsilon_w) - \epsilon_w^2(\epsilon_w^{-1} - \epsilon_\beta^{-1})] \quad \text{for } O = \text{constant} \quad (9)$$

and

$$e^2 = \frac{\epsilon_0'E^2R_0^2D^*}{\mu kT(12 - 4R_0C_0 + R_0^2C_0^2)}[(\epsilon_\gamma - \epsilon_w) - \epsilon_w^2(\epsilon_w^{-1} - \epsilon_\beta^{-1})] \quad \text{for } V = \text{constant} \quad (10)$$

Finally, substituting eqs 9 and 10 into eq 6 and taking into account that the number concentration

$$N = \frac{10^3AN_AS_1}{4\pi(R_0^2 + (R_0 + D)^2)M_m} \quad (11)$$

(where A denotes the total lipid concentration in mg/mL, S_1 is the surface area occupied by a single surfactant molecule in the bilayer, M_m is the molar mass of the surfactant, and N_A is Avogadro's number), for small deformations, for example, in the so-called Kerr region, we obtain the steady-state birefringence for vesicles:

$$\Delta n_s = \frac{(2 \times 10^3)\epsilon_0'R_0^4DD^*AN_AS_1}{15\mu kTn_w M_w(R_0^2 + (R_0 + D)^2)(12 - 2R_0C_0)}[(\epsilon_\gamma - \epsilon_w) - \epsilon_w^2(\epsilon_w^{-1} - \epsilon_\beta^{-1})][(n_\gamma^2 - n_w^2) - n_w^4(n_w^{-2} - n_\beta^{-2})]E^2 \quad \text{for } O = \text{constant} \quad (12)$$

and

$$\Delta n_s = \frac{(2 \times 10^3)\epsilon_0'R_0^4DD^*AN_AS_1}{15\mu kTn_w M_w(R_0^2 + (R_0 + D)^2)(12 - 4R_0C_0 + R_0^2C_0^2)}[(\epsilon_\gamma - \epsilon_w) - \epsilon_w^2(\epsilon_w^{-1} - \epsilon_\beta^{-1})][(n_\gamma^2 - n_w^2) - n_w^4(n_w^{-2} - n_\beta^{-2})]E^2 \quad \text{for } V = \text{constant} \quad (13)$$

In the electrooptic literature, electric birefringence in the low-field region is usually expressed in terms of the Kerr constant K, defined as

$$K = \lim_{E\to 0}\left(\frac{\Delta n}{nE^2}\right) \quad (14)$$

or in terms of the specific Kerr constant K_{sp}, defined as

$$K_{sp} = \lim_{E\to 0}\left(\frac{\Delta n}{nC_vE^2}\right) \quad (15)$$

where n denotes the refractive index of the solution and $C_v \approx V_1N$ is the volume fraction of the solute with $V_1 = 4\pi(R_0 + D)^2/3$ being the volume of a single vesicle. Thus, K and K_{sp} become for O = constant

$$K = \frac{(2 \times 10^3)\epsilon_0'R_0^4DD^*AN_AS_1}{15\mu kTn_w^2M_w(R_0^2 + (R_0 + D)^2)(12 - 2R_0C_0)}[(\epsilon_\gamma - \epsilon_w) - \epsilon_w^2(\epsilon_w^{-1} - \epsilon_\beta^{-1})][(n_\gamma^2 - n_w^2) - n_w^4(n_w^{-2} - n_\beta^{-2})] \quad (16)$$

$$K_{sp} = \frac{2\epsilon_0'R_0^4DD^*}{5\mu kTn_w^2(R_0 + D)^3(12 - 2R_0C_0)}[(\epsilon_\gamma - \epsilon_w) - \epsilon_w^2(\epsilon_w^{-1} - \epsilon_\beta^{-1})][(n_\gamma^2 - n_w^2) - n_w^4(n_w^{-2} - n_\beta^{-2})] \quad (17)$$

For V = constant, we find

$$K = \frac{(2 \times 10^3)\epsilon_0'R_0^4DD^*AN_AS_1}{15\mu kTn_w^2M_w(R_0^2 + (R_0 + D)^2)(12 - 4R_0C_0 + R_0^2C_0^2)}[(\epsilon_\gamma - \epsilon_w) - \epsilon_w^2(\epsilon_w^{-1} - \epsilon_\beta^{-1})][(n_\gamma^2 - n_w^2) - n_w^4(n_w^{-2} - n_\beta^{-2})] \quad (18)$$

$$K_{sp} = \frac{2\epsilon_0'R_0^4DD^*}{5\mu kTn_w^2(R_0 + D)^3(12 - 4R_0C_0 + R_0^2C_0^2)}[(\epsilon_\gamma - \epsilon_w) - \epsilon_w^2(\epsilon_w^{-1} - \epsilon_\beta^{-1})][(n_\gamma^2 - n_w^2) - n_w^4(n_w^{-2} - n_\beta^{-2})] \quad (19)$$

Application to Experimental Data

For illustration of the utility of the model, in the part of the Results and Discussion entitled "Extent of Deformation" we will calculate the axial ratio of vesicles by using previously published[16] steady-state electric birefringence experimental data. The selected data were obtained without the presence of added electrolyte (NaCl), and the observed electric birefringence was always positive. Here, we summarize the relevant original data (Table 1) and briefly review the experimental conditions under which those data were obtained.

Typical reproducibility of the measurements was $\pm 1.125 \times 10^{-7}$. For more details about results and plots of the actual electric birefringence signals please refer to ref 16.

Preparation and Characterization of Vesicles. The preparation and characterization of DOPC vesicles have been described in detail previously.[14] The lipid 1,2-dioleoyl-*sn*-glycero-3-phosphocholine (DOPC, from Avanti Polar Lipids; molar mass = 786.12 g) was used without further purification. Initially, large multilamellar vesicles (MLV; lipid concentration 4 mg/mL) were obtained by hydrating the dried lipid film in double-deionized and distilled water by vortex mixing (Vortex-2 Genie) for 5 min. The MLV suspension was repeatedly extruded (Extruder, Lipex Biomembranes) in five passes under nitrogen (overpressure of 3.4 bar) through two stacked polycarbonate filters of 0.2 μm pore size to produce large unilamellar vesicles

TABLE 1: Dependence of the Specific Steady-State Electric Birefringence $\Delta n_s/A$ of DOPC Vesicles on Applied Electric Field Strength (from ref 16)

applied electric field strength kV/cm	specific steady-state electric birefringence $\Delta n_s/A$, mL/mg	
0.85	(3.013×10^{-7})	
1.68	(4.197×10^{-7})	
2.50	(4.978×10^{-7})	
3.34	(5.139×10^{-7})	
4.17	5.623×10^{-7}	steady state reached
5.05	5.758×10^{-7}	steady state reached
5.80	5.865×10^{-7}	steady state reached
6.66	(6.350×10^{-7})	
7.31	(7.561×10^{-7})	

(LUV).[32] This procedure has been previously confirmed through the extent of quenching of ^{31}P NMR signal by manganese ions to produce unilamellar DOPC vesicles of narrow size distribution.[14,33] The supernatants of the centrifuged solutions were used in the subsequent light scattering and electric birefringence experiments. The mean hydrodynamic diameter $\langle D_h \rangle$ of freshly prepared monodisperse DOPC vesicles was determined by dynamic light scattering (Brookhaven model BI-200 SM) to be 193 ± 6 nm.[16] The vesicles were stable for at least 3 days as judged from the unvarying results of dynamic light scattering and electric birefringence measurements. The steady-state positive electric birefringence was found to be linearly proportional to the lipid concentration up to 0.5 mg/mL. The linear dependence suggests the absence of any contributions arising from intervesicle interactions or multiple light scattering. Dilute aqueous suspensions (0.25 mg DOPC/mL) of the vesicles were used for determination of the steady-state birefringence Δn_s.

Instrumentation. The electric birefringence instrument has been described elsewhere.[7] A 10 mW He−Ne laser (Melles-Griot, wavelength $\lambda = 632.8$ nm) was used as a light source. The optical detection system included a quarter-wave plate, with its slow axis oriented at $3\pi/4$ relative to the direction of the applied electric field **E**. The signal from the photomultiplier was recorded by a digital oscilloscope (Hewlett-Packard, model 54510A) and transferred to a computer. The electric birefringence Δn ($\equiv n_{\parallel} - n_{\perp}$) was calculated from the experimentally measured optical retardation δ through $\Delta n = \delta\lambda/2\pi L$, where $L = 5$ cm is the optical path length in the Kerr cell (with a $d = 2.5$ mm gap between the plane parallel electrodes). The observed value of Δn was corrected for the induced retardation of the cell windows ($\delta_w < 0.5°$) and for stray light. The up to ± 2 kV high-voltage rectangular pulses with rise and fall times of <100 ns were generated by a pulse generator (Cober, model 605P). To obtain the steady-state value of the birefringence, the duration of the single electric pulses was varied from 1 ms at high electric field strength up to 10 ms at low field strength. The reversing-pulse electric birefringence method was used,[16] where a sequence of two rectangular electric pulses of opposite polarity are applied to the system and the induced electric birefringence is monitored.

Vesicle preparation, dynamic light scattering, and electric birefringence experiments were carried out at 25 °C, well above the phase transition temperature ($T_c = -20$ °C)[34] of the DOPC bilayer.

Results and Discussion

Although we derived general equations for the extent of field-induced deformation (e^2, eqs 9 and 10), birefringence (Δn_s, eqs 12 and 13), the Kerr constant (K, eqs 16 and 18), and the specific Kerr constant (K_{sp}, eqs 17 and 19) in both the constant surface area (O) and constant volume (V) approximations, our interest is in the constant surface area cases. Notice, however, that since for bilayer membranes composed of two identical homogeneous layers the spontaneous curvature $C_0 = 0$,[31] the two approximations yield identical results.

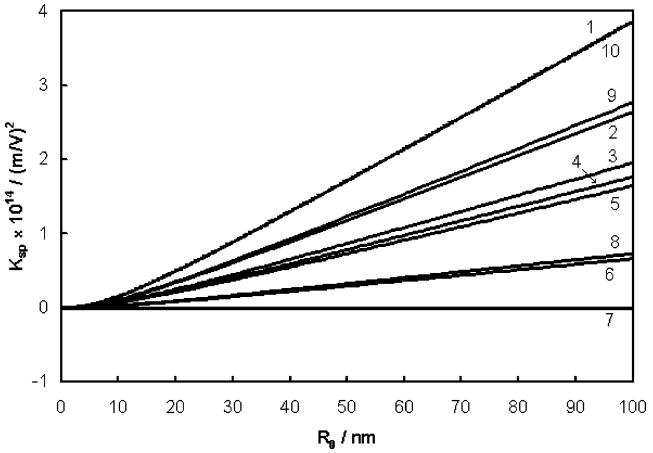

Figure 2. Calculated specific Kerr constant K_{sp} of optically isotropic vesicles ($n_\beta = n_\gamma = n_m$) as a function of their inner radius R_0 at different test values of the refractive index of the membrane: (1) $n_m = 1.5$; (2) $n_m = 1.47$; (3) $n_m = 1.45$; (4) $n_m = 1.444$; (5) $n_m = 1.44$; (6) $n_m = 1.4$; (7) $n_m = 1.333\ 35$; (8) $n_m = 1.2667$; (9) $n_m = 1.2067$; (10) $n_m = 1.1852$.

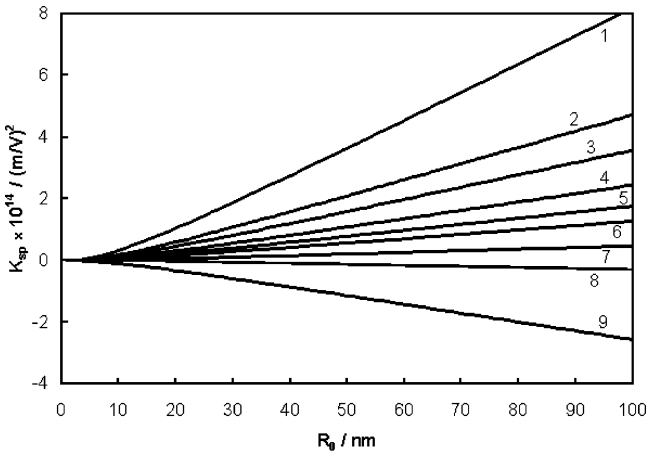

Figure 3. Calculated specific Kerr constant K_{sp} of optically anisotropic vesicles as a function of their inner radius R_0 at various test values of the refractive indexes of the membrane ($n_\beta \neq n_\gamma$): (1) $n_\beta = 1.444$, $n_\gamma = 1.5$; (2) $n_\beta = 1.444$, $n_\gamma = 1.47$; (3) $n_\beta = 1.444$, $n_\gamma = 1.46$; (4) $n_\beta = 1.444$, $n_\gamma = 1.45$; (5) $n_\beta = 1.444$, $n_\gamma = 1.444$; (6) $n_\beta = 1.45$, $n_\gamma = 1.444$; (7) $n_\beta = 1.46$, $n_\gamma = 1.444$; (8) $n_\beta = 1.47$, $n_\gamma = 1.444$; (9) $n_\beta = 1.5$, $n_\gamma = 1.444$.

In the following, we first explore the properties and predictions of the equations derived, then use the experimentally determined birefringence to calculate the extent of elongation of DOPC vesicles.

To investigate their sensitivity to the various parameters, the specific Kerr constant K_{sp} and steady-state birefringence Δn_s were calculated for different values of the electrical and optical properties of the lipid bilayer, and the results are depicted in Figures 2−5. Unless otherwise specified, the following values typical for DOPC vesicles were used in the calculations: initial inner radius $R_0 = 92.3$ nm; bilayer thickness $D = 4.2$ nm; surface area of a single surfactant molecule in the bilayer $S_1 = 7 \times 10^{-19}$ m^2;[35] axial ratio for the deformed vesicles $P = a/b = 1.05$; molar mass of the surfactant $M_m = 786.12$ g/mol; total lipid concentration $A = 0.25$ mg/mL; dielectric constant of water $\epsilon_w = 80.1$;[36] normal (ϵ_β) and tangential (ϵ_γ) components of the dielectric constant of the bilayer $\epsilon_\beta = 2$ and $\epsilon_\gamma = 2$ (typical

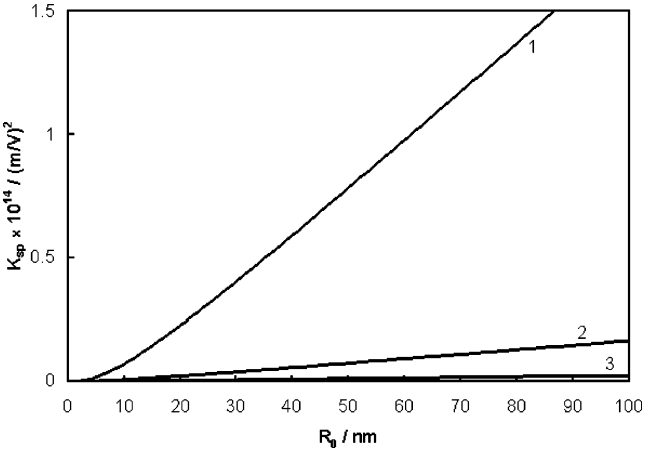

Figure 4. Calculated specific Kerr constant K_{sp} of optically and electrically isotropic vesicles ($n_\beta = n_\gamma = n_m = 1.444$, $\epsilon_\beta = \epsilon_\gamma = \epsilon_m$) as a function of their inner radius R_0 at different test values of the dielectric constant of the membrane: (1) $\epsilon_m = 2$; (2) $\epsilon_m = 15$; (3) $\epsilon_m = 40$.

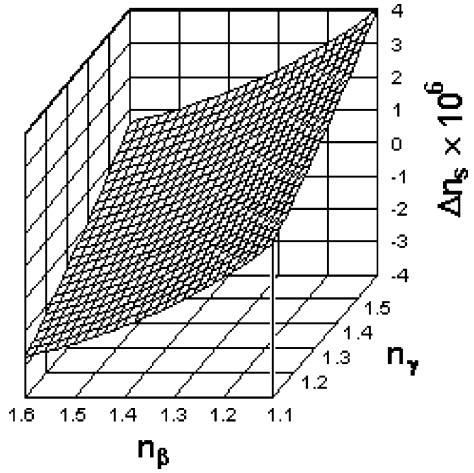

Figure 5. Calculated steady-state electric birefringence Δn_s as a function of the optical anisotropy of the membrane at small degree of deformation ($P = a/b = 1.05$) and constant vesicle concentration.

value for hydrocarbons); refractive index of water $n_w = 1.333\,35$;[36] normal (n_β) and tangential (n_γ) components of the refractive index of the bilayer $n_\beta = 1.444$ and $n_\gamma = 1.444$ (typical value for the corresponding hydrocarbon 1-octadecene);[36] spontaneous curvature of the bilayer $C_0 = 0$;[31] the dimensionless constant $\mu = 0.5$; temperature $T = 293.15$ K; dielectric permeability of vacuum $\epsilon_0' = 8.85 \times 10^{-12}$ C^2 N^{-1} m^{-2}, Boltzmann constant $k = 1.38 \times 10^{-23}$ J/K; Avogadro's number $N_A = 6.022 \times 10^{23}$ mol^{-1}.

Optically Isotropic Membrane. Figure 2 displays the specific Kerr constant calculated for optically isotropic vesicles ($n_\beta = n_\gamma = n_m$) as a function of vesicle size at constant vesicle number concentration of $N = 5.98 \times 10^{17}$ m^{-3} (corresponding to 0.25 mg/mL DOPC). As expected, K_{sp} is always positive[24,27] and increases with vesicle size. No birefringence is observed when the refractive indexes of the bilayer and the solvent are equal. The birefringence increases with the relative difference in the refractive indexes of the bilayer and the solvent. The same value of the birefringence can be observed at two different values of n_m. According to eq 6, if n_{m1} is a value of the membrane refractive index, the same birefringence will also be observed for a membrane with a refractive index n_{m2} provided that $n_{m2} = n_w^2/n_{m1}$.

Optically Anisotropic Membrane. The specific Kerr constant calculated for vesicles with an optically anisotropic membrane ($n_\beta \neq n_\gamma$) is shown in Figure 3. K_{sp} increases with the vesicle size, reaching an asymptotic linear dependence for large vesicles similar to the isotropic case. Positive and negative birefringence is possible depending on the degree of optical anisotropy of the membrane.

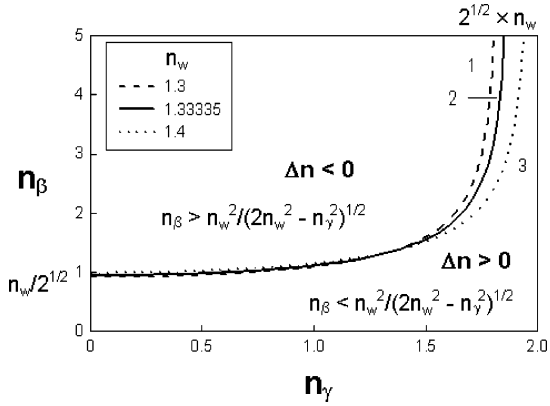

Figure 6. Plot of eq 20, for which the electric birefringence is zero despite the deformation of the vesicles. The effect of the refractive index of the solvent is shown: (1) $n_w = 1.3$; (2) $n_w = 1.333\,35$; (3) $n_w = 1.4$. The areas of positive and negative birefringence and the asymptotic values at low n_γ and at high n_β are indicated.

Isotropic Dielectric Membrane. The effect of the dielectric properties of the membrane on K_{sp} is displayed in Figure 4. We assumed that the membrane is an isotropic dielectric ($\epsilon_\beta = \epsilon_\gamma = \epsilon_m$). Three different values for ϵ_m were used in the calculations. $\epsilon_m = 2$ is a value typical for hydrocarbons and could represent an approximation of the backbone of the surfactant molecules. This value, however, does not reflect the presence of the polar groups on the two lipid/water interfaces. A better approximation is to view the membrane as a single homogeneous layer with an *effective* dielectric constant ϵ_m. Values of ϵ_m can be calculated from time-domain dielectric spectroscopy experimental data.[37] In the case of DOPC vesicles, the calculations give $\epsilon_m \sim 40$ in deionized water and $\epsilon_m \sim 15$ in 5 mM NaCl.[37] Figure 4 suggests that K_{sp} is expected to increase with the ionic strength of the solution (decreasing ϵ_m). This is in contrast with the results for solid particles where experiments have indicated that K_{sp} decreases with the ionic strength.[27]

Isotropic Electric Polarizability. The steady-state birefringence Δn_s calculated for vesicles with isotropic electric polarizability ($\epsilon_\beta = \epsilon_\gamma$) is shown in Figure 5 as a function of the membrane's optical anisotropy. Large positive birefringence is observed for $n_\beta < n_\gamma$. Negative birefringence could also be observed for small n_γ and large n_β. According to eq 12 (or 13), the vesicle system will exhibit no induced birefringence when

$$n_\beta = \frac{n_w^2}{\sqrt{2n_w^2 - n_\gamma^2}} \tag{20}$$

even if the vesicles are elongated. Plots of eq 20 for different values of the solvent's refractive index (n_w) are shown in Figure 6. For illustrative purpose, a large range of possible values of the refractive indexes n_γ and n_β is considered. Analysis of eq 20 reveals that it has the following asymptotes: $n_\beta \rightarrow n_w/\sqrt{2}$ at small values of n_γ and $n_\gamma \rightarrow \sqrt{2}n_w$ at large values of n_β. The electric birefringence will always be positive if $n_\beta < n_w^2/\sqrt{2n_w^2 - n_\gamma^2}$. The effect of the value of the solvent's refractive

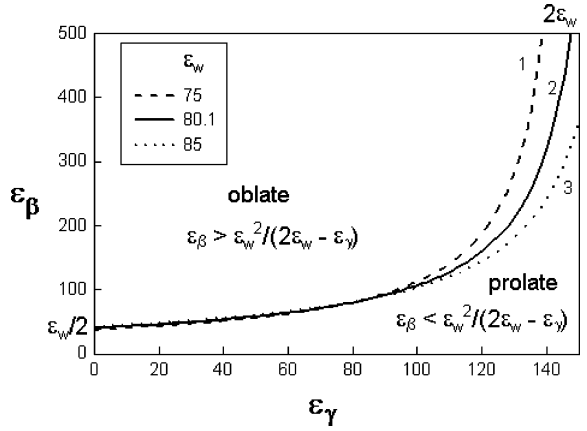

Figure 7. Plot of eq 21 for which the vesicles are not deformed by the applied electric field. The effect of the dielectric constant of the solvent is shown: (1) $\epsilon_w = 75$; (2) $\epsilon_w = 80.1$; (3) $\epsilon_w = 85$. The areas of prolate and oblate deformation and the asymptotic values at low ϵ_γ and at high ϵ_β are indicated.

index (n_w) on the sign of the electric birefringence can also be seen from the diagram.

Anisotropic Electric Polarizability. The anisotropy of the electric polarizability of the membrane plays an important role in determining the direction of the deformation of the vesicle and, consequently, of the sign of the electric birefringence. The theory presented here assumes only deformations to a prolate ellipsoid; thus, it cannot be used directly to describe the electric birefringence resulting from deformation to an oblate ellipsoid. Nevertheless, analysis of eq 12 shows that for a certain anisotropy of the dielectric constants expressed as

$$\epsilon_\beta = \frac{\epsilon_w^2}{2\epsilon_w - \epsilon_\gamma} \tag{21}$$

and substituted into eqs 5 and 5′, the polarizabilities of the vesicle will become equal ($\alpha_\parallel = \alpha_\perp$), which is also the case of a spherical vesicle. In such a case, due to the contribution of the curvature-elastic energy, the total energy of the vesicle will be minimum if the eccentricity $e = 0$. This in fact would correspond to a nondeformed spherical vesicle that will exhibit no birefringence, that is, $\Delta n_s = 0$. Analysis of the plot of eq 21 at several different values of the dielectric constant of the solvent ϵ_w (Figure 7) reveals two asymptotes: $\epsilon_\beta \rightarrow \epsilon_w/2$ at small values of ϵ_γ and $\epsilon_\beta \rightarrow 2\epsilon_w$ at large values of ϵ_β. Vesicles will always deform into a prolate ellipsoid if $\epsilon_\beta < \epsilon_w^2/(2\epsilon_w - \epsilon_\gamma)$. No deformation (and consequently no induced birefringence) is expected if eq 21 holds. If $\epsilon_\beta > \epsilon_w^2/(2\epsilon_w - \epsilon_\gamma)$, vesicles will deform to an oblate ellipsoid, but the exact value of the electric birefringence cannot be predicted because of the initial limitation imposed on the model. Here it should be noted that the actual sign of the electric birefringence depends on both the electrical and optical polarizability of the membrane, so either positive or negative birefringence could be observed for prolate as well as for oblate ellipsoidal deformations.

Extent of Deformation. The effects of lipid concentration, salt concentration, electric pulse strength, and so forth, on the amplitude and transients of the electric birefringence response are discussed in detail in refs 14 and 16. The calculations presented here are intended as an example of the use of our theoretical model for analysis of the experimental data (Table 1).

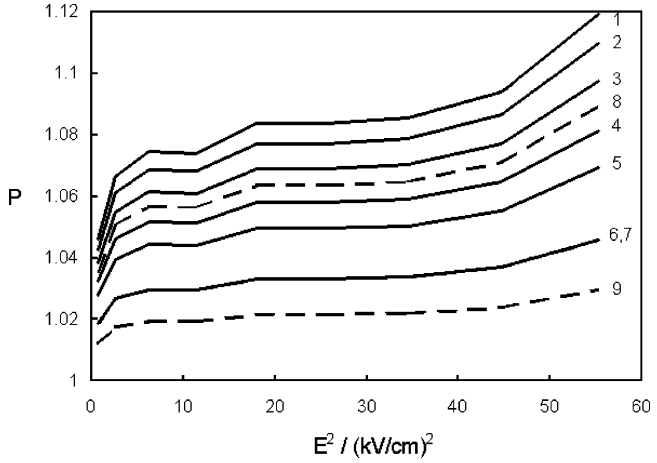

Figure 8. Axial ratio $P = a/b$ calculated from experimentally measured values of the steady-state electric birefringence of 0.25 mg/mL DOPC vesicles. The following values for the refractive indexes of the membrane were used in the calculations: (1) $n_\beta = n_\gamma = 1.44$; (2) $n_\beta = n_\gamma = 1.444$; (3) $n_\beta = n_\gamma = 1.45$; (4) $n_\beta = n_\gamma = 1.46$; (5) $n_\beta = n_\gamma = 1.47$; (6) $n_\beta = n_\gamma = 1.5$; (7) $n_\beta = n_\gamma = 1.1852$; (8) $n_\beta = 1.523$, $n_\gamma = 1.499$; (9) $n_\beta = 1.4944$, $n_\gamma = 1.5133$.

The degree of deformation, that is, the eccentricity e or the axial ratio $P = a/b = 1/(1 - e^2)^{1/2}$, to a prolate ellipsoid of the vesicles can be calculate through eq 6 from experimentally measured values of the electric birefringence Δn_s if the refractive indexes of the membrane are known. To illustrate the effect of the optical properties of the membrane, several different values of the refractive indexes n_γ and n_β were tested in the calculations. The results obtained at different applied field strengths **E** are displayed in plots of P versus E^2 (Figure 8). Clearly, P increases with E. If the membrane is assumed to be optically isotropic with a refractive index equal to that of the hydrocarbon backbone of the DOPC molecules ($n_m = 1.444$), we obtain for the axial ratio P values in the 1.07−1.09 range. Birefringence of the same magnitude could also be obtained at an axial ratio in the range of only 1.03−1.04 if the difference between the refractive indexes of the solvent and the membrane is larger ($n_m = 1.5$ or 1.1852). A better approximation for the optical properties of the DOPC bilayer is to invoke values obtained through independent measurements and calculations. Thus, we prefer the following values for the refractive indexes: $n_\beta = 1.523$ and $n_\gamma = 1.499$ as obtained from ellipsometric measurements on DSPC (the saturated analogue of DOPC) monolayer;[38] or $n_\beta = 1.4944$ and $n_\gamma = 1.5133$ as theoretically calculated for the C_{37} saturated hydrocarbon chain.[39] With these parameters, the calculated P values fall in the range of 1.02−1.07. Evidently, the accuracy of the calculated degree of deformation depends on the optical parameters available. Nonetheless, our calculated range of $P = 1.02-1.07$ is comparable with the axial ratio of $P = 1.1$ estimated by others from electric field-induced turbidity measurements on 100 nm diameter vesicles at 20 kV/cm.[11] If their P is rescaled[20] to our vesicle size (193 nm) and to a field strength of 6 kV/cm which is close to the maximum we used, one obtains $P = 1.065$, indicating a satisfactory correspondence.

The model presented here could also be used to calculate the elastic modulus κ of the bilayer from *experimentally* determined values of the specific Kerr constant K_{sp} or the Kerr constant K. For this purpose, again, both the electrical and optical properties of the vesicle membrane must be known. Efforts to determine the specific Kerr constant of DOPC vesicles will be undertaken in our laboratory.

Summary

The electric field-induced birefringence of lipid vesicles with an optically and electrically anisotropic membrane is modeled for a small extent of deformation of the originally spherical shape of the bilayer shell. Only the intrinsic birefringence of the membrane and any form birefringence of the aqueous compartment of the vesicles, caused by their field-induced elongation to a prolate ellipsoid with its major axis a parallel to the applied field **E**, are taken into account. The theory reveals the possible values of refractive indexes and dielectric constants of the membrane for which the birefringence should be either positive, zero, or negative. The sign of the electric birefringence depends on both the electrical and optical anisotropy of the membrane, so either positive or negative birefringence could be observed for prolate as well as for oblate ellipsoidal deformations. The presented model allows us to calculate the degree of elongation of the vesicles from experimental electric birefringence Δn_s data. If reasonable values for the membrane's refractive indexes are assumed, the deformation of unilamellar bilayer DOPC vesicles is found to correspond to an axial ratio P of only 1.02−1.07. The elastic modulus of the bilayer κ could also be calculated from experimental data of the Kerr constant provided the electrical and optical properties of the vesicle membrane are known.

Acknowledgment. This work was supported in part by the Welch Foundation, the National Science Foundation, and the Petroleum Research Fund of the American Chemical Society.

References and Notes

(1) O'Konski, C. T. In *Transport by Proteins*, FEBS Symposium 58, Konstanz, July 9−15, 1978; Blauer, G., Sund, H., Eds.; W. de Gruyter: Berlin, 1978; pp 237−240.

(2) Takezoe, H.; Yu, H. *Biochemistry* **1981**, *20*, 5275−5281.

(3) Takezoe, H.; Yu, H. *Biophys. Chem.* **1982**, *14*, 205−216.

(4) Ruderman, G.; Jennings, B. R.; Dean, R. T. *Biochim. Biophys. Acta* **1984**, *776*, 60−64.

(5) Borkovec, M.; Eicke, H.-F. *Chem. Phys. Lett.* **1988**, *147*, 195−202.

(6) Borkovec, M.; Eicke, H.-F. *Chem. Phys. Lett.* **1989**, *157*, 457−461.

(7) Tekle, E.; Ueda, M.; Schelly, Z. A. *J. Phys. Chem.* **1989**, *93*, 5966−5969.

(8) Würtz, J.; Hoffmann, H. *J. Colloid Interface Sci.* **1995**, *175*, 304−317.

(9) Correa, N. M.; Schelly, Z. A. *J. Phys. Chem. B* **1998**, *102*, 9319−9322.

(10) Correa, N. M.; Schelly, Z. A. *Langmuir* **1998**, *14*, 5802−5805.

(11) Neumann, E.; Kakorin, S.; Toensing, K. *Faraday Discuss.* **1998**, *111*, 111−125.

(12) Kakorin, S.; Redeker, E.; Neumann, E. *Eur. Biophys. J.* **1998**, *27*, 43−53.

(13) Schelly, Z. A. In *Handbook of Microemulsion Science and Technology*; Kumar, P., Mittal, K. L., Eds.; Marcel Dekker: New York, 1999; pp 437−456.

(14) Asgharian, N.; Schelly, Z. A. *Biochim. Biophys. Acta* **1999**, *1418*, 295−306.

(15) Hubert, D. H. W.; Cirkel, P. A.; Jung, M.; Koper, G. J. M.; Meuldijk, J.; German, A. L. *Langmuir* **1999**, *15*, 8849−8855.

(16) Peikov, V.; Schelly, Z. A. *J. Phys. Chem. B* **2001**, *105*, 5568−5574.

(17) Milner, S. T.; Safran, S. A. *Phys. Rev. A* **1987**, *36*, 4371−4379.

(18) Helfrich, W. *Z. Naturforsch. C* **1974**, *29*, 182.

(19) Winterhalter, M.; Helfrich, W. *J. Colloid Interface Sci.* **1988**, *122*, 583−586.

(20) Kummrow, M.; Helfrich, W. *Phys. Rev. A* **1991**, *44*, 8356−8360.

(21) Hyuga, H.; Kinosita, K., Jr.; Wakabayashi, N. *Jpn. J. Appl. Phys.* **1991**, *30*, 1141−1148.

(22) Hyuga, H.; Kinosita, K., Jr.; Wakabayashi, N. *Jpn. J. Appl. Phys.* **1991**, *30*, 1333−1335.

(23) Hyuga, H.; Kinosita, K., Jr.; Wakabayashi, N. *Jpn. J. Appl. Phys.* **1991**, *30*, 2649−2656.

(24) Peterlin, A.; Stuart, H. A. *Z. Phys.* **1939**, *112*, 129−147.

(25) Van der Linden, E.; Geiger, S.; Bedeaux, D. *Physica A* **1989**, *156*, 130−140.

(26) Helfrich, W. *Phys. Lett.* **1973**, *43A*, 409−410.

(27) Fredericq, E.; Houssier, C. *Electric Dichroism and Electric Birefringence*; Clarendon Press: Oxford, 1973.

(28) Lange, B.; Aragón, S. R. *J. Chem. Phys.* **1990**, *92*, 4643−4650.

(29) Böttcher, C. J. F. *Theory of Electric Polarization*, 2nd ed. (revised); Elsevier: Amsterdam, 1973.

(30) Van der Linden, E. Ph.D. Dissertation, University of Leiden, Leiden, The Netherlands,1990.

(31) Seifert, U.; Lipowsky, R. In *Handbook of Biological Physics. Volume 1A. Structure and Dynamics of Membranes*; Lipowsky, R., Sackmann, E., Eds.; Elsevier: Amsterdam, 1995; p 403−463.

(32) Mayer, L. D.; Hope, M. J.; Cullis, P. R. *Biochim. Biophys. Acta* **1986**, *858*, 161−168.

(33) Hope, M. J.; Bally, M. B.; Webb, G.; Cullis, P. R. *Biochim. Biophys. Acta* **1985**, *812*, 55−65.

(34) *Avanti Polar Lipids Products Catalog*; Avanti Polar Lipids, Inc.: Alabaster, AL; Vol. VI, p 170.

(35) Johnson, S. M. *Biochim. Biophys. Acta* **1973**, *307*, 27−41.

(36) Weast, R. C., Ed. *CRC Handbook of Chemistry and Physics*, 70th ed.; CRC Press: Boca Raton, FL, 1990.

(37) Asgharian, N. Ph.D. Dissertation, University of Texas at Arlington, Texas, 1999.

(38) Ducharme, D.; Max, J.-J.; Salesse, C.; Leblanc, R. M. *J. Phys. Chem.* **1990**, *94*, 1925−1932.

(39) Huang, W.; Levitt, D. G. *Biophys. J.* **1977**, *17*, 111−128.